

# Robust DC-Bus Voltage Control for Batteryless Brackish Water Reverse Osmosis Desalination Prototype Operating with Variable Wind and Solar Irradiation

Wahib KHIARI\*<sup>‡</sup>, Mehdi TURKI\*\*, Jamel BELHADJ\*\*\*

\*Université de Tunis El Manar, LR 11 ES 15, Laboratoire des Systèmes Electriques, Ecole Nationale d'Ingénieurs de Tunis, BP 37 – 1002, Tunisie

\*\*Université de Jendouba, Ecole Supérieure des Ingénieurs de Medjez El Bab, 9070, Tunisie

\*\*\*Université de Tunis, Ecole Nationale Supérieure d'Ingénieurs de Tunis, BP 56 – 1008, Tunisie

(wahib.khiari@gmail.com, mehdi\_turki1@yahoo.fr, Jamel.Belhadj@esstt.rnu.tn)

<sup>‡</sup>Corresponding Author; Wahib KHIARI, Laboratoire des Systèmes Electriques, Ecole Nationale d'Ingénieurs de Tunis BP 37 – 1002 Tunisie, Tel: +216 26 802 230, wahib.khiari@gmail.com

*Received: 17.04.2018 Accepted: 23.06.2018*

**Abstract-** In this paper we present a DC-Bus voltage control strategy elaborated to manage electrical power transfer for desalination system coupled to hybrid source (PV-Wind) via DC-Bus without using electrochemical storage. Reverse Osmosis (RO) technology is used to produce freshwater in this desalination system. The power control strategy elaborated called Power Field Oriented Control (PFOC) allows simultaneously the control of DC-Bus voltage and electrical power flow transfer from hybrid source to centrifugal motor-pump used for desalination. Experimental results issued from implementation of the proposed control are presented and compared to simulation results. A critical discussion is detailed to evaluate performance and effectiveness of the global system.

**Keywords** RO desalination, hybrid renewable source (PV-Wind), PFOC strategy, three-phase centrifugal motor-pump, practical implementation.

## 1. Introduction

Reverse Osmosis (RO) desalination has become a technologically and economically viable solution to tackle the challenges associated with increasing water shortages existing in many regions of the world [1-3]. Use of autonomous desalination units fed with renewable energy sources offer a promising solution particularly at isolated areas where there is no access to hydraulic and electrical grid. Coupling complementary renewable source "PV-Wind" to RO desalination offers a sustainable source of freshwater [4-8]. However, using batteries with renewable energy sources greatly increases investment and maintenance costs and have a negative impact on the environment especially for remote areas where there is a lack of adequate recycling

facilities. Therefore, several researchers are studying and evaluating batteryless desalination systems and focus on the development of robust control systems and reliable energy management strategies. B. S. Richards et al. [9-12] investigated the effect of wind speed and solar irradiance fluctuations on the performance of a brackish water desalination system. G. L. Park et al. [13] studied the potential of supercapacitors to expand the safe operating window of a wind powered RO membrane system. J. A. Carta et al. [14] presented a small-scale seawater desalination plant designed to adapt the electrical energy consumption depending on the available power from wind turbine. A control system is used to manage the number of membranes to be operational and regulate the operating pressure and feed water flow through solenoid valves.

In the present work, an experimental desalination prototype with capacity of 300 l/h was designed to evaluate different control strategies and to analyse electrical power transfer from electrical power source to motor-pumps [15]. Power Field Oriented Control (PFOC) strategy was elaborated to enhance voltage stability of the global system. This control will be applied to motor-pumps through voltage inverters to ensure RO desalination operation. This strategy allows also the control of DC-Bus voltage stability without using batteries which is a necessary condition for the correct operation of Maximum Power Point Tracking (MPPT) algorithms used with hybrid renewable sources (PV-Wind) [16-18]. Experimental analysis of variable wind and solar irradiation are studied and compared to simulation results.

## 2. PV/Wind RO Desalination System Design

A standard RO desalination unit (Fig.1) consists of several RO membranes mounted in racks, a pressurization system consisting of high pressure multistage centrifugal motor-pumps, a water lifting system formed by low pressure boosting motor-pumps, a set of pre-treatment and post-treatment filters and an energy recovery system.

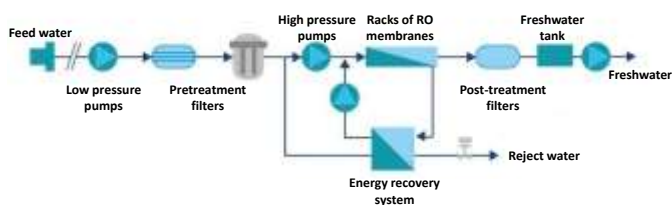


Fig. 1. RO desalination unit synoptic.

Sizing of desalination unit is based primarily on the quantity and quality of treated water to be produced. Sizing of various actuators will depend on RO membranes used. The choice of membrane type and configuration to be used for their association will depend on the nature of water to be desalinated and on the quantity and quality of desired treated water.

Designed prototype (Fig.2) uses hybrid power source (1kW Wind Generator and 1kW Photovoltaic Generator) to feed a small-scale Brackish Water Reverse Osmosis (BWRO) unit. Economical, technical and environmental analyses have shown the inconveniences of using batteries in small scale systems [19, 20]. For these reasons storage batteries have been eliminated from this prototype. Main components of the prototype are renewable energy power source, three converters interconnected via a DC-Bus, a high pressure centrifugal multi-stage three-phase motor-pump (Table 1.) and a spiral RO filtration membrane mounted in module (Table 2.).

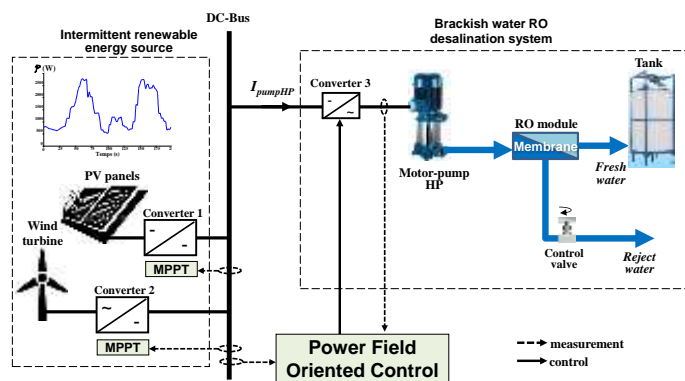


Fig. 2. Global system architecture.

Table 1. Motor-Pump-HP characteristics

Model	EBARA EVM2 22F/2.2
Rated power	2200 W
Rated voltage	230 V
Rated current	8.71 A
Rated frequency	50 Hz
Rated speed	2860 tr/min
Rated flow	20-60 l/min
Rated pressure	8.2-18.6 bar

Table 2. RO membrane parameters

Diameter	4"
Area	8 m <sup>2</sup>
Minimum salt rejection	99.7 %
Freshwater nominal flow	4.5 l/min
Maximum operating pressure	21 bar
Maximum recovery rate	20%
Maximum water temperature	45°C
Brackish water pH range	2-11

### 2.1. PV/Wind Hybrid source configuration

The main advantage of using hybrid (PV-Wind) power source is energy availability [21]. This allows the presence simultaneously of two different power sources with high efficiency, less space requirement and continuous power generation. Both power sources (Wind and PV) should be designed to operate at their maximum output power levels for any wind, temperature and solar irradiation. The hybrid system structure is presented in Fig.3.

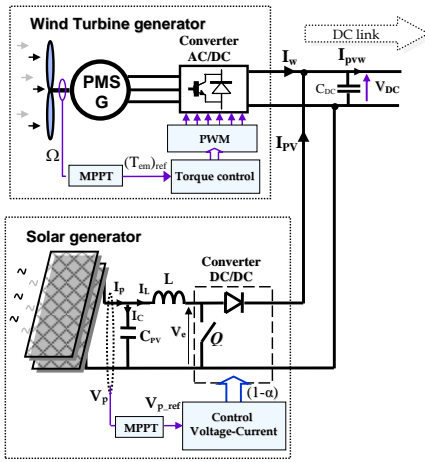


Fig. 3. Structure of hybrid power source.

Wind generator is based on a direct driven Permanent Magnet Synchronous Generator (PMSG) associated to a PWM rectifier [22]. The PMSG with a high number of pole pairs is convenient for such applications because of its capability to operate at low speed without decreasing efficiency which avoid the use of gearbox. Power characteristics of wind turbines are nonlinear. This is particularly true for vertical-axis turbines where provided power is very sensitive to the load. Thus, controlling operating point is critical to optimize energetic behaviour. Output torque  $T_w$  of wind turbine is calculated using the following equation [23]:

$$T_w = P_w / \omega_m = 0.5 \cdot \rho \cdot S \cdot R \cdot V_w^2 \cdot C_p(\lambda) / \lambda \quad (1)$$

Where  $T_w$  is the output torque of wind turbine (N.m),  $P_w$  is the mechanical power of wind turbine (W),  $\omega_m$  is the rotor mechanical speed (rad/s),  $\rho$  is the air density ( $\text{kg/m}^3$ ),  $S$  is the surface of the turbine blades ( $\text{m}^2$ ),  $R$  is the blade radius,  $V_w$  is the average wind velocity (m/s),  $C_p(\lambda)$  is the power coefficient and  $\lambda$  is the tip speed ratio given by:

$$\lambda = \omega_m \cdot R / V_w. \quad (2)$$

To maximize power extraction from the PMSG it is adequate to optimize the Torque / Current ratio. Using Field Oriented Control (FOC) and Pulse Width Modulation (PWM) voltage source rectifier it is possible to autopilot the wind generator to control the torque with high bandwidth using  $I_{sq}$  current (Fig.4).

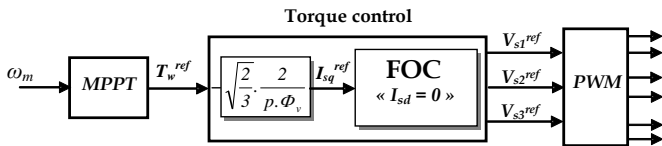


Fig. 4. Control strategy of wind turbine generator.

Regarding PV source, DC/DC converter is used with MPPT. In this case, output voltage is adjusted to optimal value allowing the transfer of maximum power to the load. Reference operating voltage  $V_{p}^{ref}$  is calculated using the following relation:

$$V_p^{ref} = K_v \cdot V_{oc} \quad (3)$$

Where  $K_v$  is the fill factor of the generator given by:

$$K_v = P_m / (V_{oc} \cdot I_{sc}) \quad (4)$$

$P_m$  is the maximum power point power,  $V_{oc}$  is the open circuit voltage and  $I_{sc}$  is the short circuit current.

The duty cycle coefficient  $\alpha$  is obtained using a cascade Voltage-Current control. A boost converter is used at the output of the PV generator to be compatible with the fixed DC link value (Fig.5).

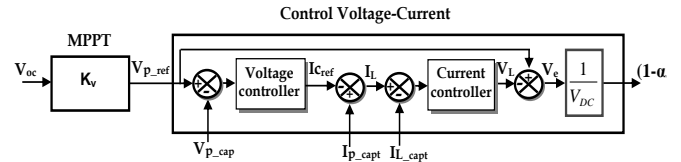


Fig. 5. Control strategy of PV generator.

It is important to notice here that for wind and PV generators MPPT technique cannot be applied unless the DC-Bus voltage is hold fixed to a constant value, hence the importance of PFOC which stabilizes the DC-Bus without the use of storage battery.

## 2.2. Reverse osmosis desalination process configuration

High pressure motor-pump (motor-pump-HP) is used to increase feed water pressure supplied to RO membrane. When applied pressure is higher than osmotic pressure, freshwater permeates across the membrane and is collected through the permeate tube, reject water is drained out (Fig.6).

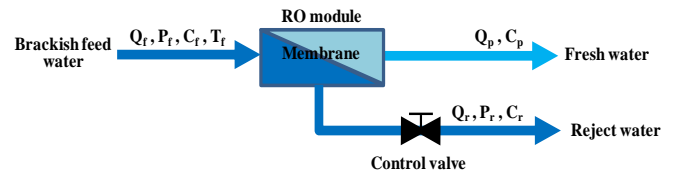


Fig. 6. Reverse osmosis process.

Where  $Q_f$  is the feed water flow (l/min),  $P_f$  is the feed water pressure (bar),  $C_f$  is the feed water salinity (mg/l),  $T_f$  is the feed water temperature ( $^{\circ}\text{C}$ ),  $Q_p$  is the freshwater flow (l/min),  $C_p$  is the freshwater salinity (mg/l),  $Q_r$  is the reject water flow (l/min),  $P_r$  is the reject water pressure (bar) and  $C_r$  is the reject water salinity (mg/l).

Equations modelling the different hydraulic quantities inside RO membrane are as follows [24]:

$$Q_p = A \cdot S \cdot (\Delta P - \Delta \pi) / d \quad (5)$$

Where  $Q_p$  is the freshwater flow across the membrane element,  $A$  is the water permeability,  $S$  is the membrane surface,  $d$  is the water density,  $\Delta P$  is the pressure drop across the membrane element and  $\Delta \pi$  is the osmotic pressure drop across the membrane element.

$$Q_r = B \cdot S \cdot \Delta C_2 / d \quad (6)$$

Where  $Q_r$  is the reject water flow across the membrane element,  $B$  is the salt permeability,  $S$  is the membrane

surface,  $d$  is the water density and  $\Delta C_2$  is the water concentration difference across the membrane element.

The water recovery rate is given by Eq. (7):

$$Y = 100 \cdot Q_p / Q_f \quad (7)$$

Mass and flow balance give the following formulas:

$$Q_f = Q_p + Q_r \quad (8)$$

$$C_r = (C_f \cdot Q_f - C_p \cdot Q_p) / Q_r \quad (9)$$

$$Q_r = Q_f - Q_p = (1 - Y) \cdot Q_f \quad (10)$$

Different types of flow configurations are possible in RO systems including single-stage, two-stage, single-pass and two-pass systems. RO systems can contain one or several groups of RO modules. Each group of module is called a stage. RO desalination systems can also have distinct RO units; each unit is called a pass. For applications where high quality of freshwater is needed, two-pass systems are usually used where feed water is treated twice in two different units. Optimization of these flow configurations can influence performances of the overall system. To increase water recovery rate, two main flow configuration options are possible: concentrate recirculation and concentrate staging.

For concentrate recirculation, the simplest module configuration is single-stage system where reject water is directly drained out. This configuration operates at a limited recovery rate that does not exceed 20 % for each membrane. To increase the overall system recovery rate, it is possible to return a portion of reject water to the supply and blend it with feed water. The concentrate recycling configuration is shown in Fig.7. The potential disadvantage of concentrate recirculation design is related to the possible need for a larger high pressure motor-pump to provide higher feed flow which implies greater energy consumption. Figure 7 shows an example schematic of a concentrate recirculation process in a single-stage RO system.

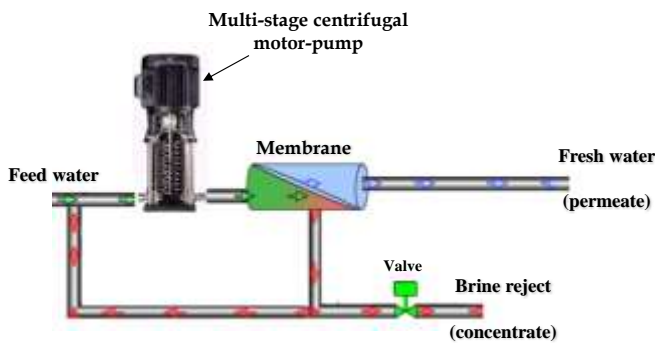


Fig. 7. Single-stage RO flow unit with concentrate recirculation.

In concentrate staging, usually multistage array of RO modules are used. Two-stage configuration is the most common configuration. In each stage, modules are connected in parallel, with respect to the direction of feed water and reject water flows. A simplified block diagram of a two-stage RO unit is shown in Fig.8. Reject water from the first stage becomes the feed water of the second stage. In this configuration, recovery rate can reach higher ratio since

reject water from the first stage is filtered again in the second stage instead of being drained out.

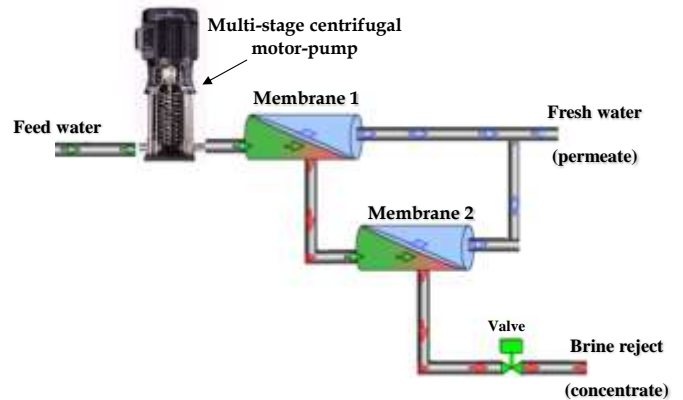


Fig. 8. Two-stage RO system.

Due to budget constraints, developed prototype is single-stage, single-pass, without recirculation. However, consideration was given to the possibility of adding membranes in the future by making the system design.

### 2.3. Power Field Oriented Control Strategy

PFOC was elaborated to control DC-Bus voltage  $V_{dc}$  and motor-pump magnetic state  $\Phi_r$  independently [25]. Using Park transformation for decoupling the flux and torque channels in Induction Motor (IM) used in motor-pumps, the transfer function on  $(d, q)$  axis can be represented by  $H(p)$ .

$$H(p) = I_{s(d,q)} / V_{s(d,q)} \quad (11)$$

$$H(p) = (1 / R_{sr}) / (1 + (\sigma \cdot L_s / R_{sr}) \cdot p) \quad (12)$$

$$R_{sr} = R_s + R_r \cdot (M_{sr} / L_r)^2 \quad (13)$$

$$\sigma = 1 - M_{sr}^2 / (L_s \cdot L_r) \quad (14)$$

Where  $R_s$  is the stator resistance,  $L_s$  is the stator inductance,  $R_r$  is the rotor resistance,  $L_r$  is the rotor inductance,  $M_{sr}$  is the mutual inductance and  $p$  is the Laplace operator.

The Rotor flux  $\Phi_r$  is calculated using a first order transfer function  $F(p)$ .

$$F(p) = M_{sr} / (1 + (L_r / R_r) \cdot p) \quad (15)$$

Where  $M_{sr}$  is the mutual inductance,  $L_r$  is the rotor inductance,  $R_r$  is the rotor resistance and  $p$  is the Laplace operator.

Rotor flux  $\Phi_r$  reference value is equal to 0.8 Wb which allows to have a good magnetization of the induction motor for a wide range of electrical power variation imposed by the control. As the PFOC is established in Park's  $(d, q)$  reference frame, IM magnetic flux is regulated by controlling  $d$  axis current  $I_{sd}$ , while DC-Bus voltage is regulated by controlling  $q$  axis current  $I_{sq}$ . This is done by virtue of power balance relationship at Voltage Source Inverter (VSI) which can be written by neglecting losses:

$$V_{dc} \cdot I_{pump} = V_{sd} \cdot I_{sd} + V_{sq} \cdot I_{sq} \quad (16)$$

On the basis of a cascade control (Fig.9 and Fig.10), it will be assumed that current internal loop dynamic is

sufficiently fast (1 ms) with respect to  $V_{dc}$  loop and rotor flux loop. Synthesis of DC voltage regulator  $R_V$  and rotor flux  $R_\phi$  regulator is carried out in the same way as current regulators  $R_I$  by adopting poles/zeros cancellation method. Response time of these external loops was chosen to be equal to 100ms.

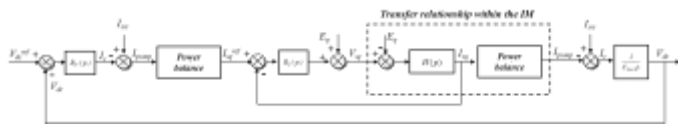


Fig. 9. Block diagram of  $V_{dc}$  control loop.

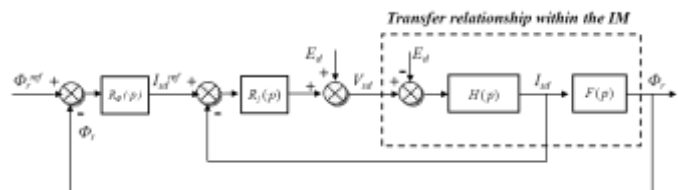


Fig. 10. Block diagram of flux control loop.

### 3. Simulation and experimental results

Mathematical models of hybrid (PV/Wind) power source, high pressure motor-pump and RO membrane was developed and simulated using Matlab software. The different parameters of the simulated system are chosen as below:

- The wind speed was chosen between 4 to 20 m/s, ambient temperature equals to 25 °C and solar irradiance is 1000 W/m<sup>2</sup>.
- The DC-Bus voltage reference value is set to 320 V.
- The motor-pump rotor flux  $\Phi_r$  reference value is set to 0.8 Wb.
- The feed water salinity of brackish water equals to 4500 ppm (4.5 g/l).
- The BWRO unit operates with a fixed recovery ratio ( $Y = 20\%$  when the motor-pump operate at nominal power).
- Elaborated control PFOC has been discretized and simulated with the whole system using a sampling period of  $5 \cdot 10^{-5}$ s.

Performances of hybrid power source MPPT control are presented in Fig.11. The peak electrical power reaches 1962W.

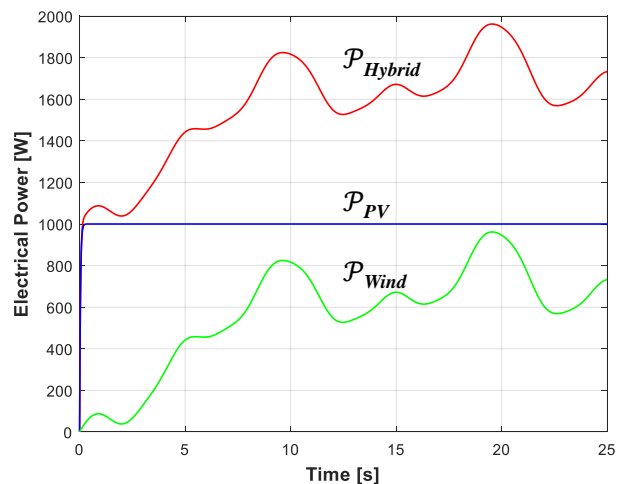


Fig. 11. Hybrid PV-Wind power source evolution.

Figure 12. shows the performances of DC-Bus voltage control insured by  $V_{dc}$  control loop of PFOC strategy (Fig.9). Reference value is set to 320 V. Simulation results show the swiftness and effectiveness of the control to stabilize DC-Bus voltage for a wide range of electrical power variation (from 1039 W to 1962 W) and this without using batteries in the system.

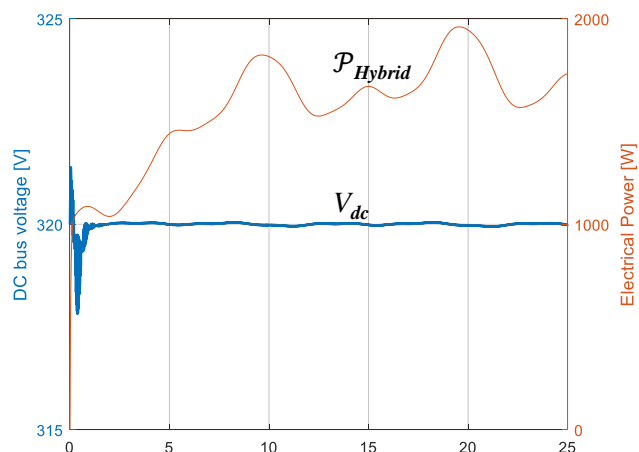
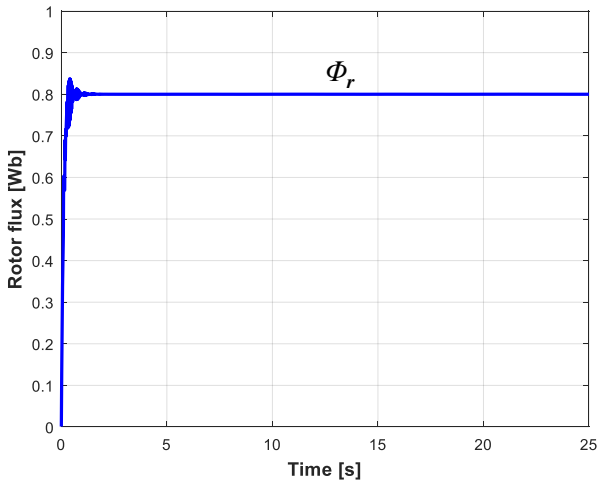


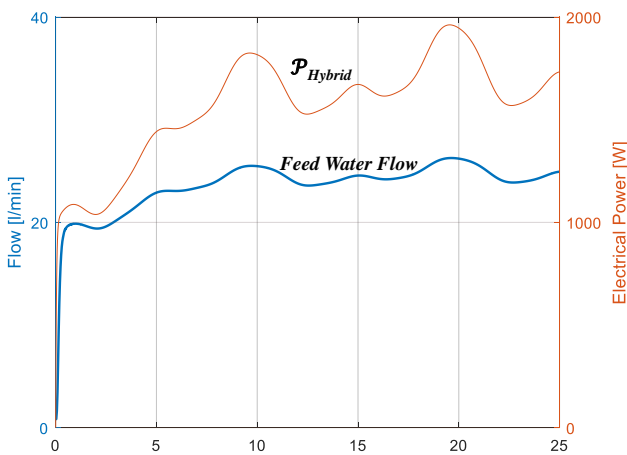
Fig. 12. DC-Bus voltage control.

Figure 13. shows performances of rotor flux  $\Phi_r$  control insured by flux control loop of PFOC strategy (Fig.10). Reference value is set to 0.8 Wb. Simulation results show the good performances of current and flux regulators to impose a constant rotor flux despite the significant variation in electrical power supply.



**Fig. 13.** Rotor flux control.

Since the high pressure motor-pump directly feeds the RO membrane, we are particularly interested in the evolution of feed water flow (Fig.14) and pressure (Fig.15) at the input of the membrane. It is noticed that these two hydraulic quantities follow the evolution of electrical power with a slower dynamics for feed water flow. For this range of electrical power variation from 1039 W to 1962 W, the feed water flow rate has undergone a variation of 19.4 l/min to 26.27 l/min and the feed water pressure a variation of 9 bar to 15.7 bar.



**Fig. 14.** Feed water flow variation.

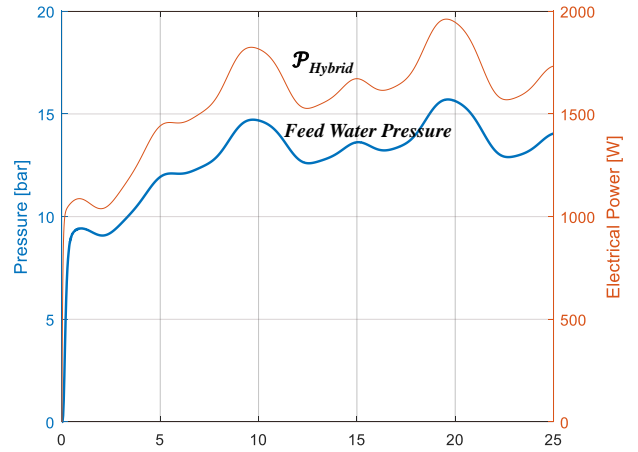


**Fig. 15.** Feed water pressure variation.

Evolution of feed water flow  $Q_f$  as well as freshwater  $Q_p$  and reject water  $Q_r$  flows across the RO membrane are shown in Fig.16. Freshwater flow rate undergoes a fluctuation of 2 l/min for 1039 W electrical power supply to 4.35 l/min for 1962 W.

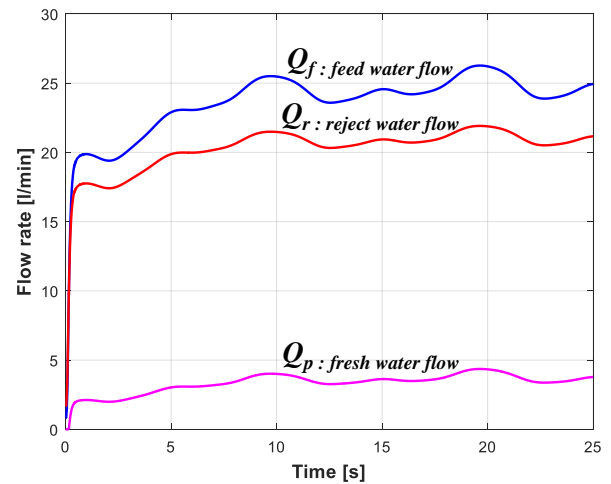


**Fig. 16.** Water flows variation across RO membrane.

To validate developed control strategy and to evaluate performances of the overall system, PFOC strategy was implemented on DSpace DS1104 control board and tested on the brackish water desalination test bench (Fig.17 and Fig.18).



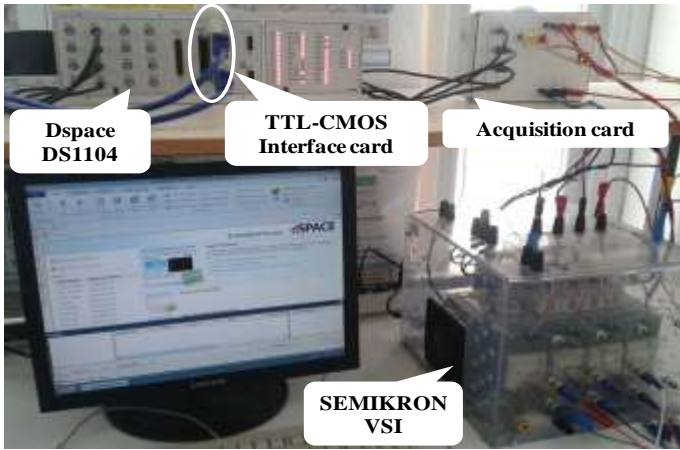


Fig. 17. Experimental environment.

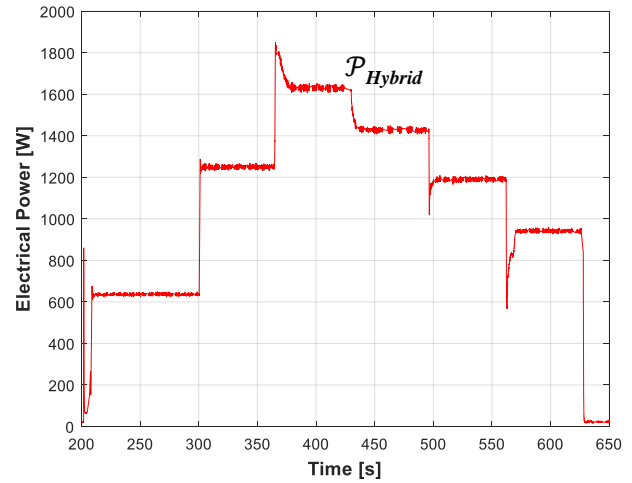


Fig. 19. Hybrid PV-Wind power source evolution.

Figure 20 shows performances of DC-Bus voltage control loop through the control of motor-pump-HP  $I_{sq}$  current. Experimental results show good performances in terms of response time and robustness to the severe test fluctuations provided by the equivalent power source. The DC-Bus voltage is maintained stable at 320 V despite variations in the electrical power source. This will allow to properly apply MPPT algorithm with PV and wind generators.

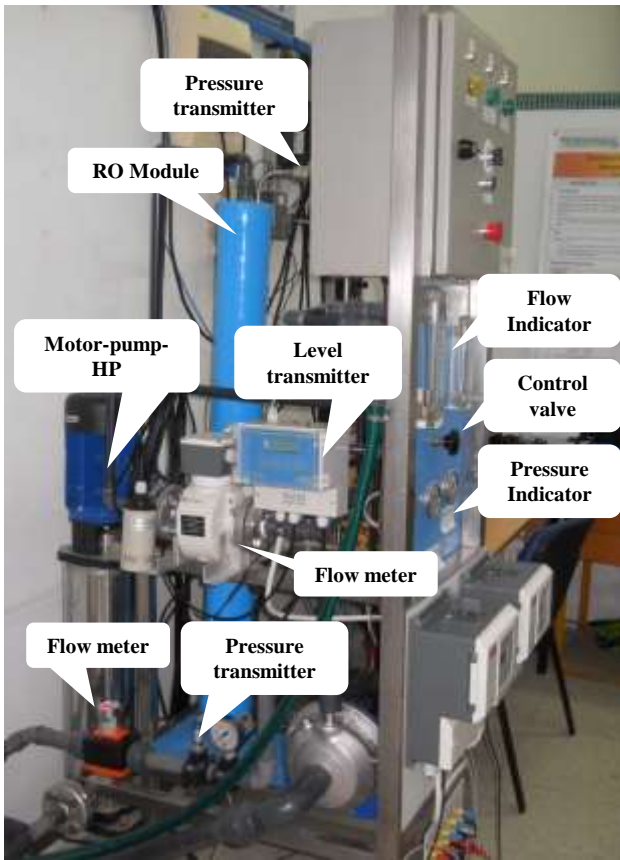


Fig. 18. Experimental test bench.

The main purpose in these experimental tests is to evaluate the robustness and swiftness of PFOC in the motor-pump control to ensure desalination process and DC-Bus stabilization face of rough variations in electrical power. For this reason, hybrid renewable source was emulated using a programmable DC power supply that can generate a variable power profile. Evolution of hybrid electrical power emulated is shown in Fig.19.

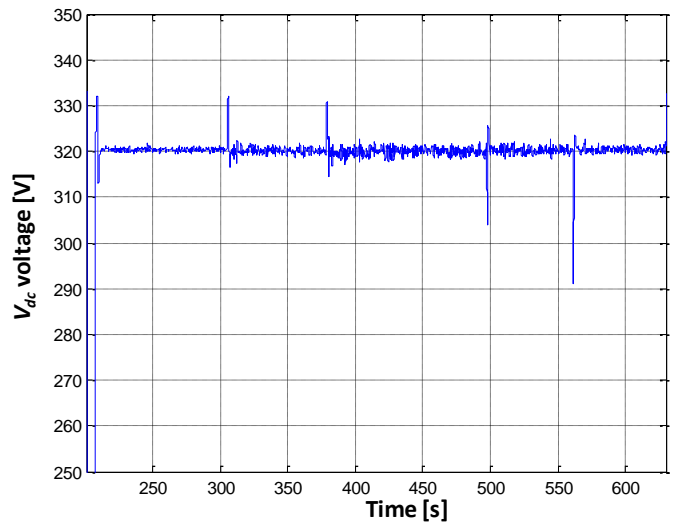


Fig. 20. DC-Bus voltage control.

Figure 21 shows performances of rotor flux control through the control of motor-pump-HP  $I_{sd}$  current.

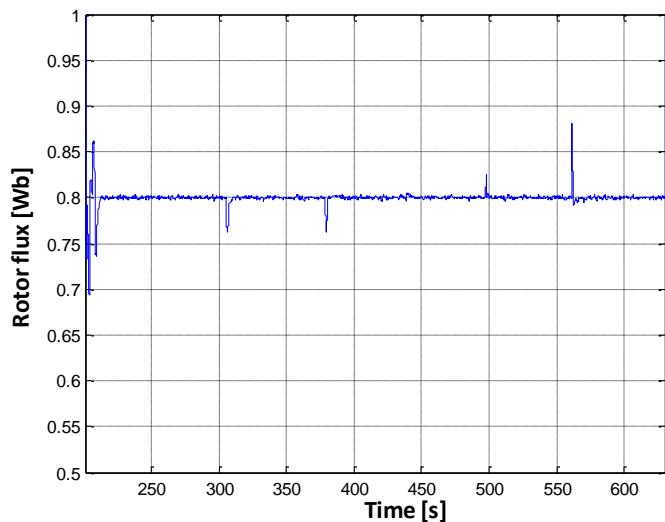


Fig. 21. Rotor flux control.

Evolution of feed water flow and pressure are shown in Fig.22. Feed water flow rate varies from 15 l/min for 630 W electrical power supply to 23 l/min for 1630 W. Feed water pressure varies from 6.6 bar to 13.2 bar for the same power range.

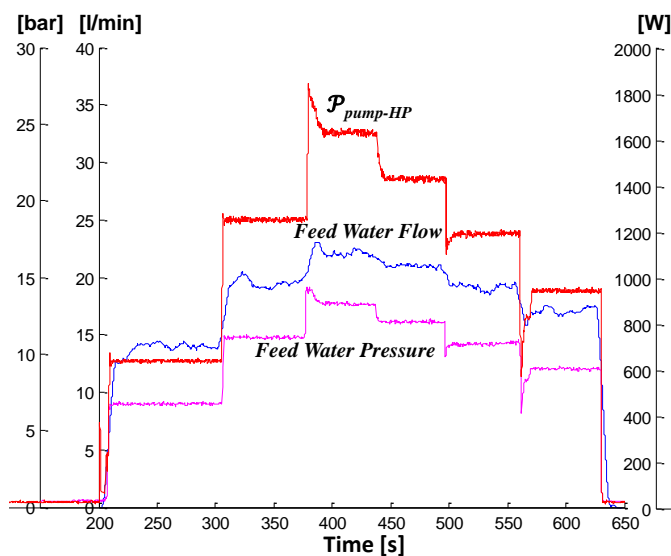


Fig. 22. Feed water flow and pressure variation.

Evolution of feed water flow, freshwater flow and reject water flow across the RO membrane are shown in Fig.23. Freshwater flow rate undergoes a fluctuation of 0.5 l/min for 630 W electrical power supply to 4.2 l/min for 1630 W.

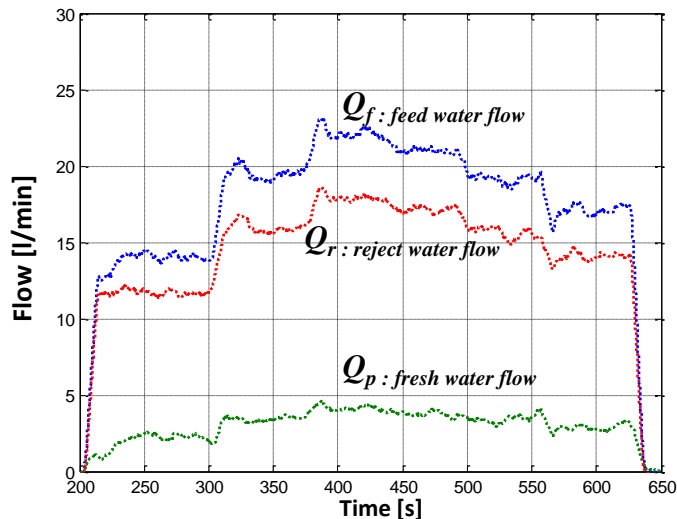


Fig. 23. Water flows variation across RO membrane.

#### 4. Conclusion

In this work we presented an experimental analysis of batteryless brackish water reverse osmosis desalination prototype operating with variable electrical power. The developed control PFOC allows simultaneously the control of DC-Bus voltage and renewable electrical power feeding high pressure motor-pump used for desalination process. The different models and control loops of the entire system were validated experimentally and simulation results show good agreement to experimental results. The importance of this control lies in its ability to keep a stable DC-Bus without using storage batteries which allows to MPPT algorithms to operate properly with PV and wind generators.

#### Acknowledgements

This work was supported by the Tunisian Ministry of Higher Education and Research under Grant LSE-ENIT-LR 11 ES15 and the European project "ERANETMED - EDGWISSE" ID 044.

#### References

- [1] A. Dubreuil, E. Assoumou, S. Bouckaert, S. Selosse, N. Maizi, "Water modeling in an energy optimization framework – The water-scarce middle east context", Appl. Energy, vol. 101, pp. 268-279, 2013.
- [2] L. F. Greenlee, D. F. Lawler, B.D. Freeman, B. Marrot, P. Moulin, "Reverse osmosis desalination: water sources, technology, and today's challenges", Water Res., vol. 43, No. 9, pp. 2317-2348, 2009.
- [3] S. Burn, M. Hoang, D. Zarzo, F. Olewniak, E. Campos, B. Bolto, et al., "Desalination techniques — A review of the opportunities for desalination in agriculture", Desalination, vol. 364, pp. 2-16, 2015.
- [4] H. Sharon, K. S. Reddy, "A review of solar energy driven desalination technologies", Renew. Sustainable Energy Rev., vol. 41, pp. 1080-1118, 2015.



- [5] N. Ghaffour, J. Bundschuh, H. Mahmoudi, M. F. A. Goosen, "Renewable energy-driven desalination technologies: A comprehensive review on challenges and potential applications of integrated systems", *Desalination*, vol. 356, pp. 94-114, 2015.
- [6] M. C. Garg, H. Joshi, "A Review on PV-RO Process: Solution to Drinking Water Scarcity due to High Salinity in Non-Electrified Rural Areas", *Separ. Sci. Technol.*, vol. 50, No. 8, pp. 1270-1283, 2014.
- [7] V. G. Gude, "Energy storage for desalination processes powered by renewable energy and waste heat sources", *Appl. Energy*, vol. 137, pp. 877-898, 2015.
- [8] M. G. Buonomenna, J. Bae, "Membrane processes and renewable energies", *Renew. Sustainable Energy Rev.*, vol. 43, pp. 1343-1398, 2015.
- [9] B. S. Richards, G. L. Park, T. Pietzsch, A. I. Schäfer. "Renewable energy powered membrane technology: Brackish water desalination system operated using real wind fluctuations and energy buffering". *Journal of Membrane Science*, vol. 468, pp. 224-232, 2014.
- [10] G. L. Park, A. I. Schäfer, B. S. Richards, "Renewable energy powered membrane technology: The effect of wind speed fluctuations on the performance of a wind-powered membrane system for brackish water desalination". *Journal of Membrane Science*, vol. 370, No. 1-2, pp. 34-44, 2011.
- [11] B. S. Richards, D. P. S. Capão, W. G. Früh, A. I. Schäfer. "Renewable energy powered membrane technology: Impact of solar irradiance fluctuations on performance of a brackish water reverse osmosis system". *Separation and Purification Technology*, vol. 156, pp. 379-390, 2015.
- [12] B. S. Richards, G. L. Park, T. Pietzsch, A. I. Schäfer. "Renewable energy powered membrane technology: Safe operating window of a brackish water desalination system". *Journal of Membrane Science*, vol. 468, pp. 400-409, 2014.
- [13] G. L. Park, A.I. Schäfer, B. S. Richards. "Renewable energy-powered membrane technology: Supercapacitors for buffering resource fluctuations in a wind-powered membrane system for brackish water desalination". *Renewable Energy*, vol. 50, pp. 126-135, 2013.
- [14] J. A. Carta, J. González, P. Cabrera, V. J. Subiela. "Preliminary experimental analysis of a small-scale prototype SWRO desalination plant, designed for continuous adjustment of its energy consumption to the widely varying power generated by a stand-alone wind turbine". *Applied Energy*, vol. 137, pp. 222-239, 2015.
- [15] W. Khiari, M. Turki, J. Belhadj, "Experimental prototype of Reverse Osmosis desalination system powered by intermittent renewable source without electrochemical storage «Design and characterization for Energy-Water management»", 2<sup>nd</sup> International Conference on Electrical Sciences and Technologies in Maghreb CISTEM, Marrakech, DOI: 10.1109/CISTEM.2016.8066819, pp. 1-7, 26-28 October 2016.
- [16] Y. Mahmoud, "Toward a Long-Term Evaluation of MPPT Techniques in PV Systems". 6<sup>th</sup> International Conference On Renewable Energy Research And Applications ICRERA, San Diego, pp. 1106-1113, 5-8 November 2017.
- [17] S.A. Rizzo, N. Salerno, G. Scelba, A. Sciacca, "Enhanced Hybrid Global MPPT Algorithm for PV Systems Operating under Fast-Changing Partial Shading Conditions". *Int. J. Renew. Energy Res. IJRER*, vol. 8, No. 1, pp. 221-229, 2018.
- [18] H. Nademi, Z. Soghomonian, L. Norum, "A Robust Predictive MPPT Strategy: An Enabler for Improving the Photovoltaic Conversion Source". 6<sup>th</sup> International Conference On Renewable Energy Research And Applications ICRERA, San Diego, pp. 1086-1091, 5-8 November 2017.
- [19] V. G. Gude, N. Nirmalakhandan, S. Deng, "Renewable and sustainable approaches for desalination". *Renewable and Sustainable Energy Reviews*, vol. 14, No. 9, pp. 2641-2654, 2010.
- [20] A. Al-Karaghoul, D. Renne, L. L. Kazmerski, "Technical and economic assessment of photovoltaic-driven desalination systems". *Renewable Energy*, vol. 35, No. 2, pp. 323-328, 2010.
- [21] J. Barzola, M. Espinoza, F. Cabrera, "Analysis of Hybrid Solar/Wind/Diesel Renewable Energy System for off-grid Rural Electrification". *Int. J. Renew. Energy Res. IJRER*, vol. 6, No. 3, pp. 1146-1152, 2016.
- [22] D., A. Thakur, "A Comprehensive Review on Wind Energy System for Electric Power Generation: Current Situation and Improved Technologies to Realize Future Development". *Int. J. Renew. Energy Res. IJRER*, vol. 7, No. 4, pp. 1786-1805, 2017.
- [23] A. Harrouz, I. Colak, K. Kayisli, "Control of A Small Wind Turbine System Application". 5<sup>th</sup> International Conference On Renewable Energy Research And Applications ICRERA, Birmingham, pp. 1128-1133, 20-23 November 2016.
- [24] S. Kumarasamy, S. Narasimhan, "Optimal operation of battery-less solar powered reverse osmosis plant for desalination". *Desalination*, vol. 375, pp. 89-99, 2015.
- [25] W. Khiari, A. B. Rhouma, M. Turki, J. Belhadj, "DSPACE implementation and experimentation of Power Field Oriented Control for motor-pump fed by intermittent renewable sources", 1<sup>st</sup> International Conference on Electrical Sciences and Technologies in Maghreb CISTEM, Tunis, DOI: 10.1109/CISTEM.2014.7077035, pp. 1-6, 3-6 November 2014.